Energy 76 (2014) 436–444

Contents lists available at ScienceDirect

Energy

journal homepage: www.elsevier.com/locate/energy

Feasibility study on thermoelectric device to energy storage system of an electric vehicle

I.-S. Suh [a,*], H. Cho [b], M. Lee [a]

[a] Korea Advanced Institute of Science and Technology, 291 Daehak-Ro, Yuseong-Gu, Daejeon 305-701, Republic of Korea
[b] Yonsei University, Seodaemun-Gu, Seoul 120-749, Republic of Korea

ARTICLE INFO

Article history:
Received 6 April 2014
Received in revised form
10 July 2014
Accepted 9 August 2014
Available online 17 September 2014

Keywords:
Electric vehicle
Thermoelectric
Waste heat recovery
Battery
Pre-heating

ABSTRACT

EVs (Electric vehicles) have garnered much of attention over the past few decades as a promising solution to greenhouse gases in transportation. In this paper, a feasibility study is performed applying a TE (thermoelectric) device to the energy storage system of an electric vehicle. By applying a TE device to the Li-family battery system, the effectiveness of the TE device for possible cooling or pre-heating of the battery, or to recover the electrical energy from the waste heat are investigated. Based on the simulated flow field and temperature distribution, the effective locations of thermoelectric devices are identified and installed, and their performances in view of heat recovery or pre-heating during winter and cooling performance during summer are evaluated by simulation. In addition, the results are verified through an experimental setup under a controlled environment of air flow and temperature. Based on the simulation and experiment, the overall effectiveness of cooling or heating, and waste heat recovery quantity is evaluated. It is found that, though the cooling or pre-heating energy is small, the functional benefit to the efficiency and charging/discharging performance of battery system can contribute significantly to sound battery operation, hence to the reliability and overall performance of EVs.

1. Introduction

The transportation sector has been a top contributor to GHG (global greenhouse gas) emissions. EVs (Electric vehicles) have garnered considerable attention over the past few decades as a promising solution to global GHG (global greenhouse gas) emissions. A thermoelectric generator or TEG (thermoelectric generator) is a device that converts waste heat into electricity. Recently, it became very popular as a method of improving fuel economy and total efficiency of either ICE (internal combustion engine) driven vehicles or electric vehicles. According to the U.S. DOE (Department of Energy), about 15% of the total fuel energy of ICE vehicles is consumed to run a car and its auxiliary units, but most of the other energy is transformed into heat during vehicle operation, which consequently and directly contributes to the acceleration of global warming [1]. To deal with this generation of heat, an ATEG (automotive thermoelectric generator) is a device that converts waste heat in ICE vehicle operation into electricity, and many researchers have demonstrated ATEG prototype modules achieving 40%–70% efficiency [2,3]. The lifetime of an ATEG can be 10–20 years without maintenance with low $/W installation cost. The overall vehicle fuel economy improvement has shown a 1–4% increase depending on the vehicle type [4,5].

Thermal management of batteries in EVs and HEVs (hybrid EVs) is essential for effective operation in all weather conditions because the performance and cost of EVs are directly affected by the performance (power and energy capability), lifespan, reliability, charge acceptance, and cost of batteries. Battery temperature typically increases from its initial state with active operation of charging and discharging because of internal heat generation caused by electrochemical reactions and resistance or Joule heating. Thermal management has been emphasized in the design of battery modules and packs when applied to the production of those EVs. Battery temperature affects the available discharge power and energy, as well as the charging range of accepting brake regeneration electrical energy. Battery temperature also influences the lifespan of the battery significantly.

Thus, the objective of thermal management of a battery system is to maintain the operating temperature within a range that is optimized for performance and lifespan. Each battery type works better in a particular temperature range, for example, lead-acid, NiMH (nickel metal hydride), and Li-ion (lithium ion) batteries

* Corresponding author.
E-mail address: insoo.suh@kaist.ac.kr (I.-S. Suh).

http://dx.doi.org/10.1016/j.energy.2014.08.040
0360-5442/

are operated optimally under conditions between 25 and 40 °C, and at these temperatures, they achieve a good balance between performance and lifespan [6–8].

Another objective of the thermal management of battery is to maintain even temperature distribution within a battery pack [9]. The temperature variation from module to module in a pack could cause different charge and discharge behaviors of each module, resulting in electrically unbalanced modules and packs with deteriorated overall performance as an energy storage system. For optimal operation, a temperature variation of less than 5 °C is desirable between modules. The overall heat generation rate from a battery pack during the charging and discharging process determines the required capacity of the cooling system [10]. For example, a Li-ion battery pack with 6 Ah energy storage capacity generates 12 W/cell at 0 °C, 3.5 W/cell at 22–25 °C, and 1.22 W/cell at 40–50 °C when the discharge rate is 5 C, where the C-rate is defined as the nominal current used by the battery divided by 1 h. For cooling purposes, forced air or natural convection process are frequently applied.

In this study, we will examine the effect of cooling by using a thermoelectric generator on a battery pack system. Typical thermoelectric materials with a high Seebeck effect are semiconductors with high electric conductivity and low thermal conductivity. The most common materials are Bi_2Te_3, PbTe, and SiGe, and less frequently used are *n*-type BiSb, and *p*-type TAGS and $FeSi_2$, which also have good thermoelectric properties [4]. Usually the symbol ZT represents the thermoelectric material effectiveness, and a high ZT means that the TEG can convert more heat energy into electric energy. Nissan, GM Chevy, and BMW have tested TEG in their vehicles. The primary challenge of TEG is its relatively low heat-to-electricity conversion efficiency, and research groups are attempting to improve the intrinsic conversion efficiency of thermoelectric materials, even utilizing new nano-crystalline or nanowire materials [11].

Low-temperature heat can be recovered if the cost per watt, $/W, is sufficiently low. With the recent technological developments in the TEG field, the application potential has increased. Several studies are reported to recover low-temperature heat by applying a high Seebeck coefficient of TE material or a new architectural proposal to enhance the recovered heat capacity, like inserting a space inside the TE device [9,11,12]. An extensive study about thermoelectric generators for automotive waste heat recovery systems through numerical modeling, parametric evaluation, and topologies has been reported [2,3]. Fuel cell application of waste heat recovery has been also studied in view of numerical modeling of a thermoelectric generator with a compact plat-fin heat exchanger for high-temperature PEM fuel cell exhaust heat recovery [13].

The maximum power output of the thermoelectric device, W_{max} is expressed as.

$$W_{max} = \frac{((S_p - S_n)\Delta T)^2}{4R}, \tag{1}$$

where ΔT is the temperature difference between the hot side and the cold side, R is the electrical resistance of the thermoelectric device, S is the Seebeck coefficient, and the subscripts p and n denote the p- and n-type thermoelectric semiconductors, respectively [8]. As shown in Eq. (1), large Seebeck coefficients, a large temperature difference, and low electrical resistance are required to obtain high power output.

In this paper, a combined numerical model is developed to investigate the flow and thermal field distribution for an onboard battery system and, thus, to examine a TE device's effect on battery cooling and heating, and waste heat recovery from the battery heat during operation is evaluated considering seasonal ambient temperature change. In addition, a lab-based experimental setup is developed simulating the battery room in an EV, and the effectiveness of the TE device during summer and winter has been verified in terms of cooling, pre-heating of battery start-up, and waste heat recovery. The objective of this research is graphically summarized in Fig 1.

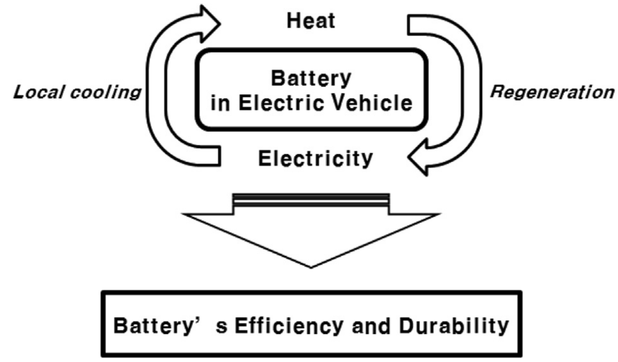

Fig. 1. Battery performance and life extension by applying thermoelectric device for thermal management while generating electric energy for an electric vehicle.

In summer, the battery operating temperature is higher than that required for optimal performance; therefore, cooling is necessary. As the localized temperature rise might cause an unbalance of cell and pack performance, it is necessary to keep uniform temperature distribution. Therefore, in this study, TE devices are placed locally in the possible hot spot area for efficient cooling of battery cells or packs, as conceptually shown in Fig. 2. The TE device does not require additional refrigerant or pumps, nor is it affected by any mechanical vibration environment, which will help the EV operating in the long range.

During the winter season, ambient temperature is lower than the battery or motor/inverter's temperature, the thermoelectric device can be used as a pre-heating device or for waste heat recovery, as in Fig. 2. As shown in Eq. (1), the recovered electrical power by TEG can be used as additional energy so that the overall efficiency can be raised. Additional consideration must be given to the fact that the TEG device can behave as a thermal insulator to the battery cells or packs, so the battery performance might be affected or degraded. Therefore, it is important to have a well-considered and optimized TE configuration based on accurate prediction of efficiency improvement by TEG and efficiency degradation due to a battery temperature increase.

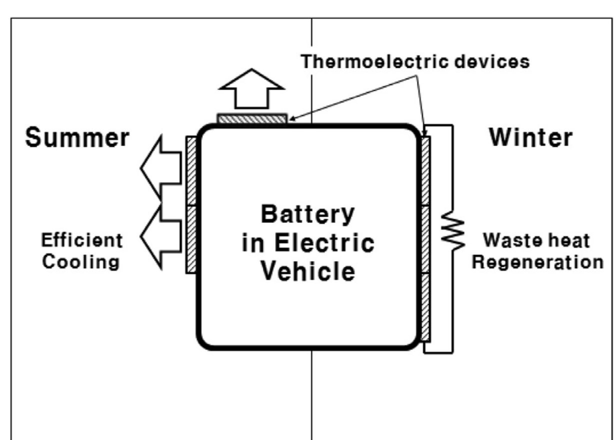

Fig. 2. TE device application concept for different seasonal requirements for an EV battery system.

Thus, in this study, the cooling effect of the battery system by a TE device during summer season, and pre-heating and waste heat recovery during winter season is simulated and optimized in view of optimal TE configuration. Reviewing the published papers in the related field, this study involves in a unique subject of applying a TE device in energy storage system of an electric vehicle. And through the flow and temperature simulation by CFD (computational fluid dynamics) techniques, the resultant effects are quantified. In addition, a simplified but controlled laboratory-based experimental test setup is designed and validated with simulation results with various ambient conditions, battery heating due to its operation, and TE activities. By applying a thermoelectric device over the battery pack surface, the cooling effectiveness during summer, and the pre-heating and waste heat recovery performance during winter have been quantified through simulation and lab-environment experiment.

The rest of this paper is organized as follows. Section 2 presents the simulation modeling of a battery room with electric vehicle specification, CFD approach and the simulation results. The experimental setup and results on the effect of TE device over the battery pack with the variation of surrounding temperature conditions of summer and winter are provided in Section 3. And conclusions are followed in Section 4.

2. Simulation of a flow field

2.1. Battery room and an EV specification

The vehicle used for this study is an electric vehicle converted from a commercial SUV type. An AC induction motor with the maximum of 60 kW and continuous output of 25 kW is applied, driven by 220 V AC, with Li-polymer battery with 320 V DC and 13 kWH energy storage capacity, as shown in Fig 3, along with interior battery room. In addition to the main power drive system, air conditioning is performed by a 1.5 kW BLDC motor and the braking system is operated by a 1.0 kW integrated vacuum pump and motor system (Fig. 4).

2.2. Flow and temperature simulation

Today CFD modeling and calculation are amply and well described in many text books [14,15] and applied routinely and

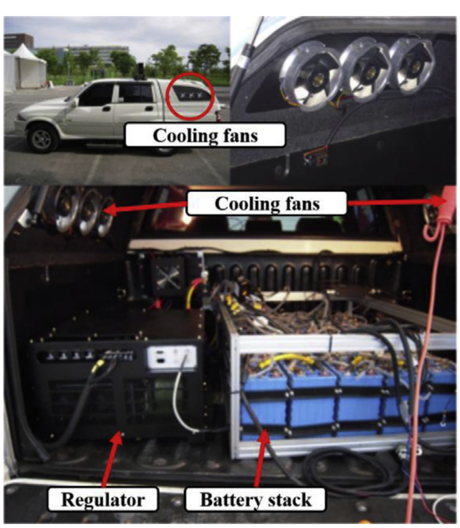

Fig. 3. An electric vehicle and battery room pictures for simulation model and TE study model.

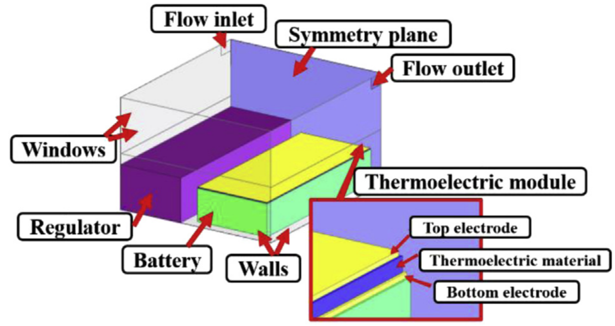

Fig. 4. Battery room model.

frequently in engineering analysis. In this paper we focus on the application of CFD as an engineering tool for flow and thermal field analysis in order to quantify the effect of TE device over a battery pack in an electric vehicle. While numerous published papers are available in developing the governing equations and in deriving efficient calculation, here we only describe the basic approach of the simulation approach. And the commercial codes CFD ACE+ [16], CFX [17], FLOW-3D [18] and FLUENT [19] are investigated for specific application area for comparison [20]. For the flow and thermal analysis, in this paper, the commercial numerical software CFD-ACE+ has been used for thermal design and analysis, which requires a heat transfer model (conduction and convection), flow field (laminar and turbulent), and electrical field (DC conduction and Seebeck effect) numerical modeling and calculation. The characteristic of indoor air motions are always difficult to identify, whether it is locally induced turbulence or transitional or fully developed turbulence. Since there is no interest in highly fluctuating turbulent motion in this case, the governing equations are time-averaged and the most extensively used turbulent transport model, $k-\varepsilon$, is employed to model the flow [21–23]. The resulting mean conservation equations can be written as follows:

$$\frac{\partial}{\partial t}(\rho\phi) = \frac{\partial}{\partial x_j}\left(\Gamma_\phi \frac{\partial \phi}{\partial x_i} - \rho U_j \phi\right) + S_\phi, \tag{2}$$

where ϕ (=1 [continuity], U, V, W, k and ε, etc.) represents any mean scalar variable or velocity component. The diffusion coefficient, Γ_ϕ, and the source term, S_ϕ, are given in Ref. [7] for three-dimensional fluid dynamic governing equations. As the boundary conditions, molecular viscosity becomes as significant as eddy viscosity ($\mu_\tau = C_\mu \rho k^2/\varepsilon$) due to the dumping effect of the walls. In such regions, the standard $k-\varepsilon$ model is not applicable and wall functions are employed in order to evaluate the velocity component parallel to the boundaries and the heat transfer at the surfaces. According to this method, the heat flux from the wall at a constant temperature can be written as

$$Q_w = c_p A(T_a - T_w), \tag{3}$$

where Q is the heat flux from the wall to the room, T_a is the air temperature in the room, A is the area, and c_p is a wall function coefficient and is computed as a function of the local flow in W/m^2 °C. To reduce the calculation time, the half of the model has been calculated with the symmetry condition. With the rectangular structured mesh, the total number of cells used is 128,464. From the physical battery room of Fig. 3, the simplified battery room model is described in Fig. 4. The overall geometry is simulated with rectangular shapes, as shown in Fig. 5, and the cooling fan at inlets and outlets are simulated with rectangle shapes, and 100 cells of the battery system are modeled as a bulk solid with internal heat

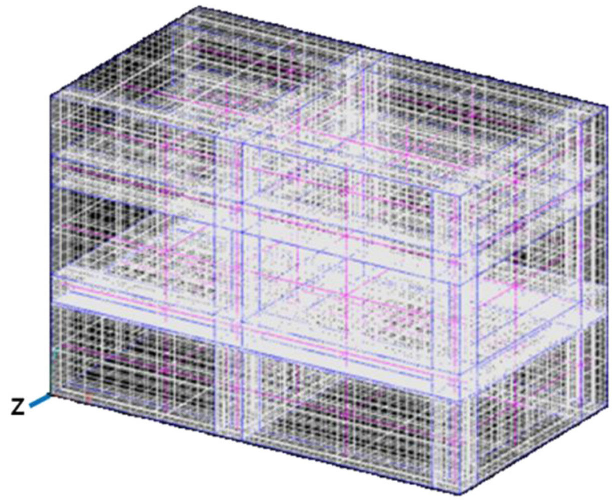

Fig. 5. Simulation domain and mesh generation.

generation of 640 W (assuming 5% of battery energy conversion efficiency), which correspond to 2.03 kW/m^2.

The effective heat transfer coefficient through the vehicle window was set as 3.33 W/m^{2}K, from the combined heat transfer coefficient of generic heat loss through the window and to the ambient air. The effective heat transfer coefficient through the side walls and the ceiling surface of the vehicle was set as 9.09 W/m^{2}K by combining the heat loss coefficient through the side wall and to the ambient air. The simulation conditions are summarized in Table 1.

2.3. TE modeling for simulation

TE devices are installed on the top surface of the battery system with a total thickness of 10 mm including upper and lower electrodes of 2 mm. Commercialized TE devices, TE20-127-12, with a Seebeck coefficient of 100 μV/K (Table 2) in the form of thermopile with several tens of n/p-type device legs in series were employed for this study. For convenience of calculation, the thermopile is modeled as a single unit with larger area and a higher Seebeck coefficient for equivalent heat calculation.

2.4. Simulation results

The simulated flow distribution is shown in Fig. 6 in terms of the local flow velocity and the streamline distribution. The inlet air for cooling flows at 8 m/s through the battery room and is discharged to the outside at the same speed.

In summer conditions with an ambient temperature of 30 °C, the temperature distribution around the battery room when operating is shown in Fig. 7. Under steady state condition, the local battery temperature shows 68.2 °C as an average and 70 °C as a maximum under 640 W of heat generation from the battery. And

Table 1
Simulation condition summary.

Items	Specification
Battery	320 V × 40 A
Battery efficiency	5%
Forced air velocity at inlet and outlet	8 m/s
Ambient temperature (summer)	30 °C
Ambient temperature (winter)	0 °C

Table 2
Physical properties for simulation.

	Density (kg/m^3)	Specific heat ((J/kg)·K)	Conductivity ((W/m)·K)	Electrical conductivity (Ω^{-1} m^{-1})	Seebeck constant (μV/K)
Air	1.164	1007	0.0263	N/A	N/A
Battery	1150	1460	5	N/A	N/A
TE material	13,546	139.6	8.5	9.6 e + 7	100
Electrode	8960	385	385	1.7 e + 8	6.5
Regulator	7900	470	48	N/A	N/A

the maximum temperature occurs at the center region of the battery pack.

With the TE devices installed on the top side of the battery, the local temperature was reduced by 0.5 °C by attaching TE devices with no electrical power to the TE device. This result is caused by the passive cooling effect due to the high thermal conductance of TE material. When the electrical power is supplied to the TE device, i.e. the active TE action case, the spatially averaged battery temperature is examined with variable input voltage levels to the TE device, as shown Fig. 8. The cooling effect due to the thermal electric property and the heating effect due to the Joule heating vary depending on the input voltage; thus, the temperature decreases with lower input voltage and increases with higher input voltage region, as in Fig. 8. Thus, it can be concluded that an optimal supplying voltage exists for the most efficient cooling performance with a given installed layout of a TE device.

In this case, when the supply voltage is 3 mV, the cooling effect is maximized with the battery temperature of 35.7 °C. The local temperature decrease is more than 30 °C with the TE device installed on the top side of the battery pack when compared with the condition without TE devices. This means that the cooling effect of the TE device during high ambient temperature season will positively help the battery thermal management, and thereby

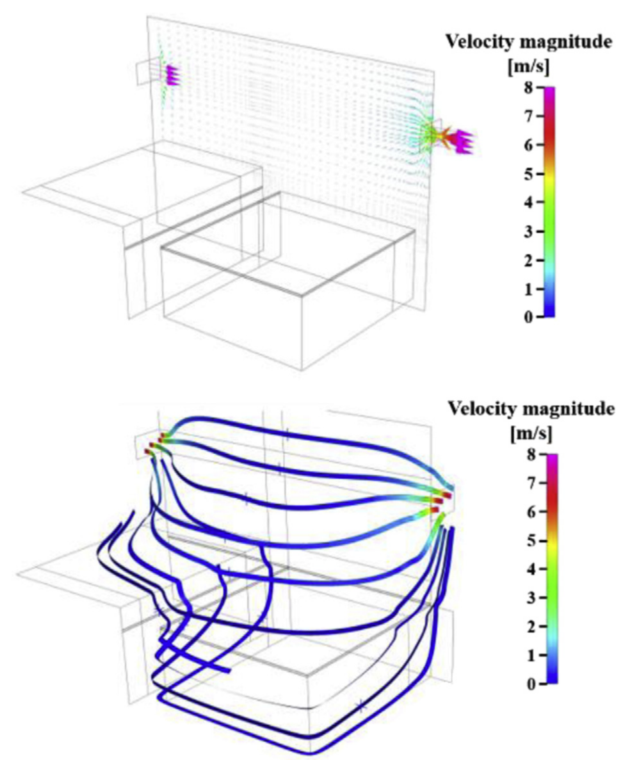

Fig. 6. Velocity and streamline distribution results from flow field simulation.

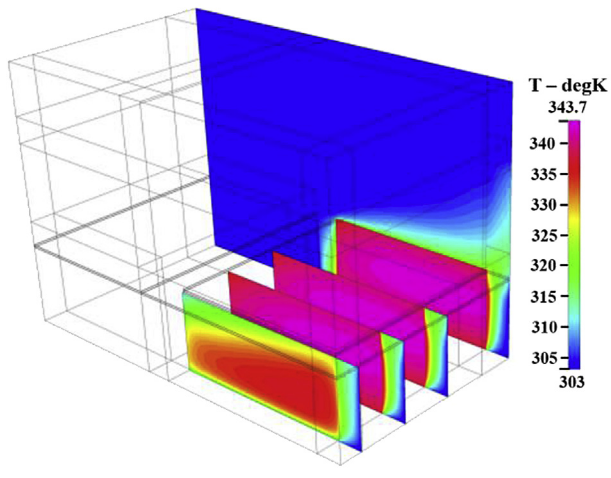

Fig. 7. Simulated temperature field distribution during summer.

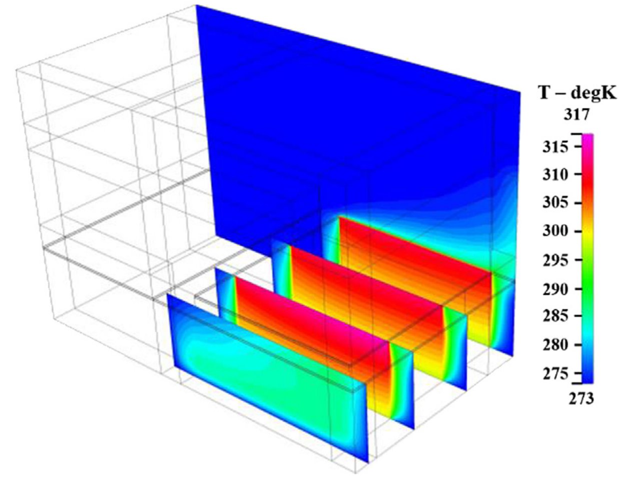

Fig. 9. Pre-heating performance with an active TE device.

battery charging and discharging capability and efficiency, and its durability. These results also indicate that the TE devices with a higher Seebeck coefficient will provide better cooling performance and efficiency.

During the cold ambient temperature environment of winter, simulated at 0 °C, the pre-heating capability before operation of the battery and waste heat recovery during battery operation are examined through the simulation. Under subzero conditions when the battery is started up, the required activation energy for the battery's chemical reaction cannot be achieved; the battery provides a lot lesser power than is required and can possibly be permanently damaged. Typically, the battery must be heated rapidly after a cold start-up at −30 °C, where it requires 5 kW of power to a temperature at which that the battery can deliver near full power discharging of 25 kW [21].

The same TE device is installed in the simulation model as in summer case. The temperature distribution inside the battery room with −3 mV of electrical supply power is shown in Fig. 9. Supplying the negative electrical power means that the efficient heating is expected on the battery side of the TE device because the TE device heats and cools simultaneously, and effective heating can be obtained by diminishing the cooling effect due to the Joule heating of the TE device.

With −3 mV of electrical supply to the TE device, the spatially averaged battery temperature reached 34.6 °C, which is an appropriate operational temperature of the battery. Since the heat from the battery is generated when operating, the required heat quantity for pre-heating will be smaller than such a case. Thus, the supply voltage can be lower than −3 mV for the practical application. By varying the input voltage to the TE device, the spatially averaged battery temperature trend is shown in Fig. 10. The required electrical energy to pre-heat the battery up to 20 °C is calculated with 400 W with 2.2 mV of electrical power supply.

Waste heat recovery during cold ambient condition is also simulated with the same installation concept as in the summer case above. The local temperature distribution inside the battery room from the simulation is shown in Fig. 11. The spatially averaged temperature is calculated as 31.6 °C and the maximum is 31.2 °C with about 30 °C temperature difference from the ambient.

The electrical field distribution results from the simulation are shown in Fig. 12 with the calculated open circuit voltage of 38.9 μV due to the temperature difference of both sides of the installed TE device, which means that the small amount of waste heat recovery is obtained without having additional heating device, thereby improving the overall energy efficiency of the system. The applied TE material for this simulation is with the Seebeck coefficient of

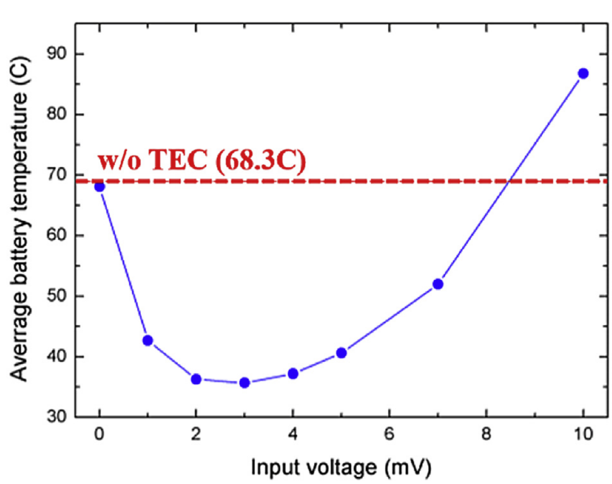

Fig. 8. Averaged battery temperature change with input voltage to a TE device for cooling action.

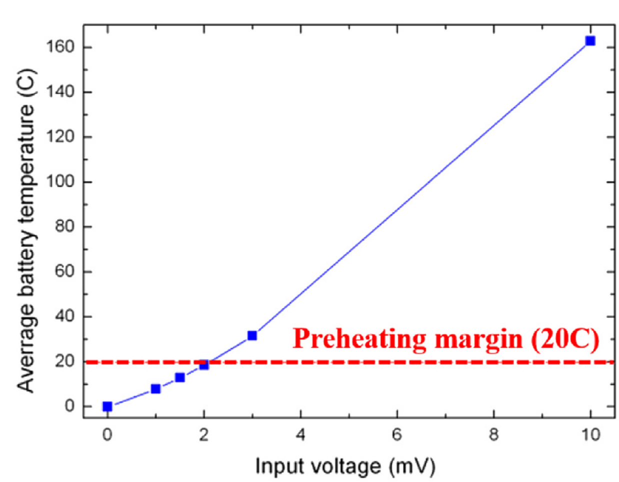

Fig. 10. Averaged battery temperature change with TE input voltage in pre-heating action.

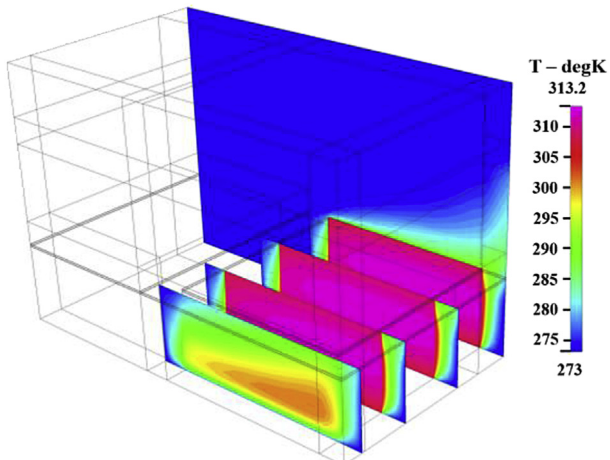

Fig. 11. Battery room temperature distribution when battery is operating under winter condition.

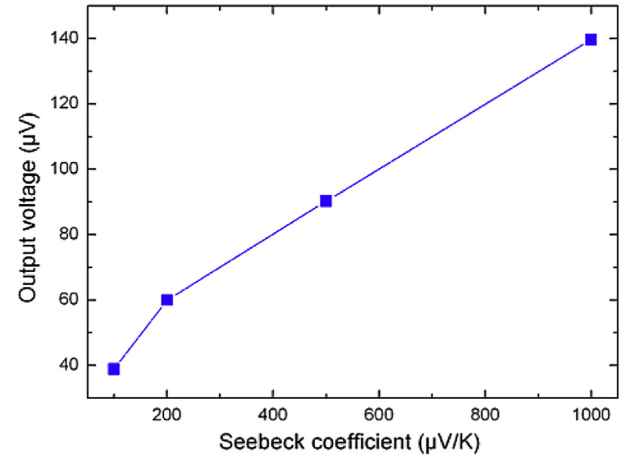

Fig. 13. Voltage generation by a TE device with different Seebeck coefficients.

100 μV/K, but the generated electrical voltage and energy can be increased with a higher Seebeck coefficient of TE material, as shown in Fig. 13.

3. Experimental setup and results

3.1. Objectives of the experimental setup

In order to verify the simulation results by deriving proper physical parameters, a simplified experimental setup has been designed and implemented in the lab-environment for controlled experiments. The battery has been modeled as a set of 20 of acrylic and 5 copper blocks, with the each block size measured as 50 mm × 50 mm × 23.7 mm. The space between the battery cells is set as 5 mm, which is 1/10 of the battery cell size. The battery model has been placed inside the duct, simulating the equivalent air flow condition with constant air velocity. To simulate the ambient temperature, the temperature in the test setup can be varied with the test conditions. For the heat generation model, a cylindrical cartridge heater with 110 W/220 V was used to supply an equivalent amount of heating as in the actual vehicle. The heater was placed in the center of a copper block, as shown in Fig. 14, where the adjacent blocks are also copper blocks to model the actual condition of heat generation inside the battery room (Fig. 15).

The bottom side of the battery model is covered with Bakelite plate and Styrofoam material for thermal insulation conditions due to their low thermal conductivity. TE device for the experiment is installed on the top of the subject copper block, and the specification of applied TE device is described in Fig. 15. In order to improve the performance of the TE device, the fin-type heat exchanger device has been added, as shown in Fig. 14. Then, the

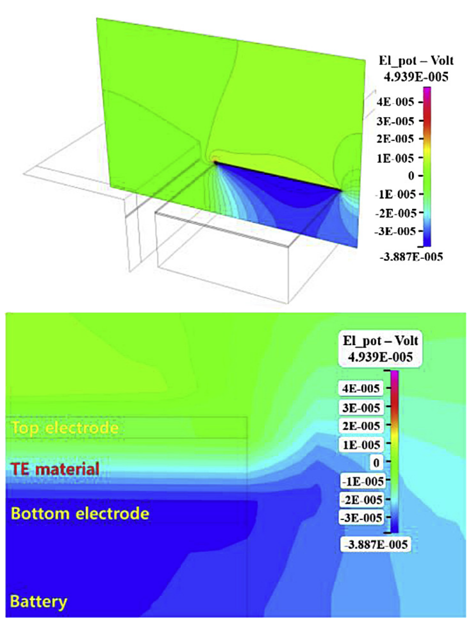

Fig. 12. Thermoelectric distribution with waste heat recovery from the battery.

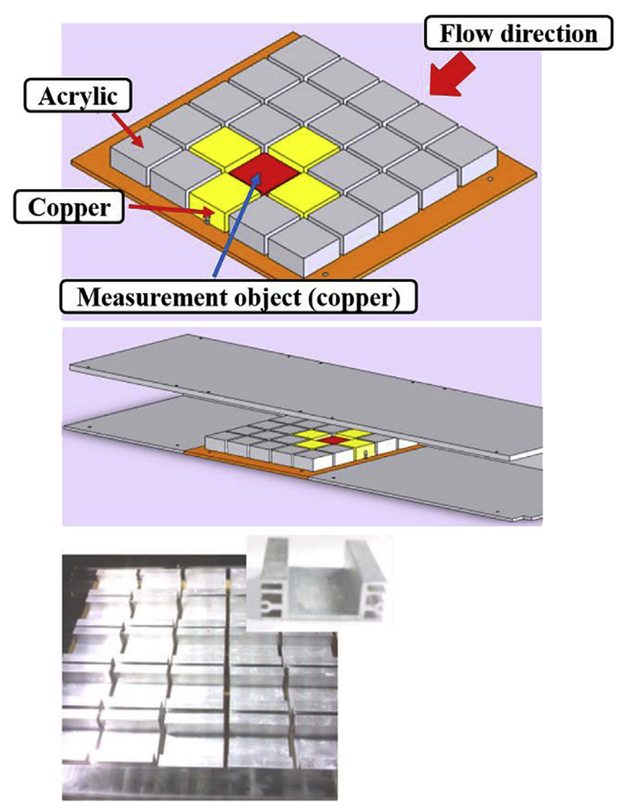

Fig. 14. Simple diagram and picture of experimental setup.

Model		TS20-127-12 (manufactured by Thermotron)
Max current		19.4 (A)
At 25°C	Max heat capacity	153.6 (W)
	Max voltage	16.2 (V)
	Max temperature	70 (°C)
Size (A×B×C×H)		50×50×50×3.7 (mm)

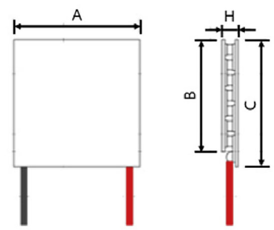

Fig. 15. Specification of a TE device used for experiment setup.

temperature over the copper block is measured with ten sets of surface thermocouples. For the real-time temperature distribution measurement, an infrared camera is placed on the top side of the battery-model block. To control the emissivity of those block surfaces, the non-reflective black film has been added for accurate infrared temperature measurement. Test conditions are summarized as follows.

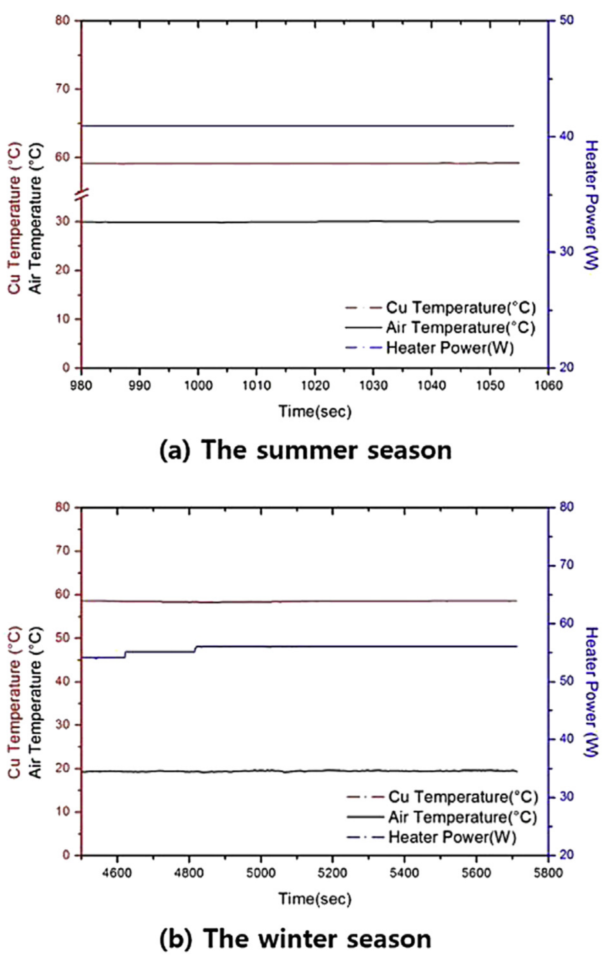

Fig. 16. Battery heat generation due to operation.

Flow condition:
- Air velocity: 1 m/sec homogeneous flow
- Ambient temperature of summer conditions: 30 °C
- Ambient temperature of winter conditions: 18–20 °C

Battery heat generation:
- Summer conditions: 40.8 W at 60 °C
- 2.2 W at 30 °C
- Winter conditions: 56.1 W at 20 °C

The actually measured temperatures of test setup components are shown in Fig. 16 to verify the simulated condition compared with the actual battery in a vehicle.

3.2. Test results of summer conditions

3.2.1. Cooling effect by the TE device

When the electrical power is supplied to the TE device, one side generates heat and the other side absorbs heat. With this property, the heating or cooling of the battery is possible. Under summer conditions, the cooling of the battery was performed to evaluate the performance of the TE device, of which results are described in Fig. 17. As observed in the simulation, there exists an optimal input electrical voltage or power. When the electrical current to TE device was varied from 0 A to 2.0 A, the temperature of the copper block dropped from 59 °C to 56 °C and then started to increase at 1.8 A. Thus, in this case, the optimal current range for cooling of the TE device is found to be between 1.6 A and 1.7 A.

Based on the observation, the cooling performance is measured with a supply current of 1.6 A, and the cooling performance results are summarized in Fig. 18. With 1.6 A of electric current supply to the TE device, the battery temperature was lowered by 2.8 °C after 180 s starting from 60 °C. After 6 min, the temperature did not drop any more, remaining at 57 °C, because the heating and cooling rates are the same and thermal equivalence condition had been reached. If a TE device with a higher Seebeck coefficient is used, the cooling performance is expected to be greater. The qualitative results in view of the existence of an efficient performance range and the reaching of steady thermal equivalent condition are expected to be similar, even with different TE materials.

With the variation of battery temperature keeping the other temperature conditions of the flow field and of the supply current to TE device the same, the cooling performance was measured. This condition can be interpreted as varying the temperature of the flow field and battery. For the case with supply current to a TE device of 1.6 A, the temperature drop is 2.8 °C when the battery temperature

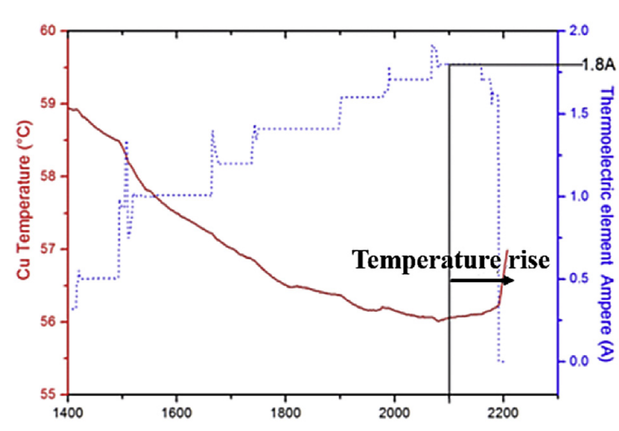

Fig. 17. Cooling performance of TE device with current variation.

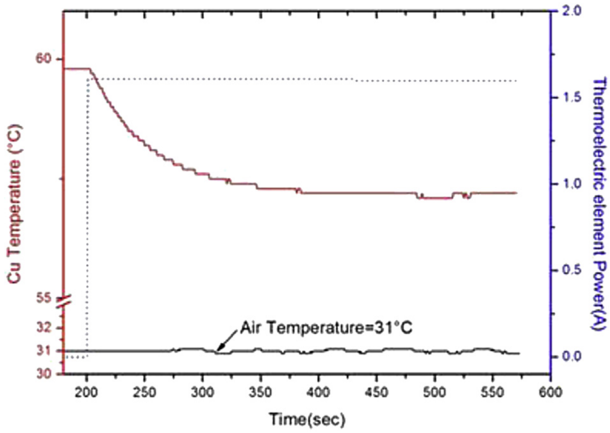

Fig. 18. Cooling performance with large temperature difference between battery and flow field.

is about 30 °C higher than the average temperature of the flow field, as shown in Fig. 19. When both temperatures are similar, the temperature drop is observed as 2.1 °C due to the cooling effect of the TE device.

3.3. *Test results of winter conditions*

3.3.1. *Test results on waste heat recovery*

For winter test conditions, the average flow field temperature is within the 18–20 °C range, lower than the battery's; thus, the TE device will have a voltage difference across both sides of the terminals. Starting from 59 °C of copper block (or battery) temperature, the voltage across TE device drops when the flow field temperature is kept at 19–20 °C. The voltage difference has been measured as 0.27 V with 30 °C difference, and 0.1 μV with 0.6 °C difference.

3.3.2. *Test results on pre-heating*

Under winter conditions, the flow field temperature can be lower than battery's optimized operating temperature. And the TE device can be used as heating source with proper control of supply current direction to the TE device, whose results are shown in Fig. 20. Starting from 22 °C of battery temperature with a 19.5 °C in flow field temperature, the battery's reach at 30 °C in 176 s and at 40 °C in 539 s, as shown in Fig. 21. In this case, the battery is assumed to be in non-operating condition, which means no additional heat generation from the battery.

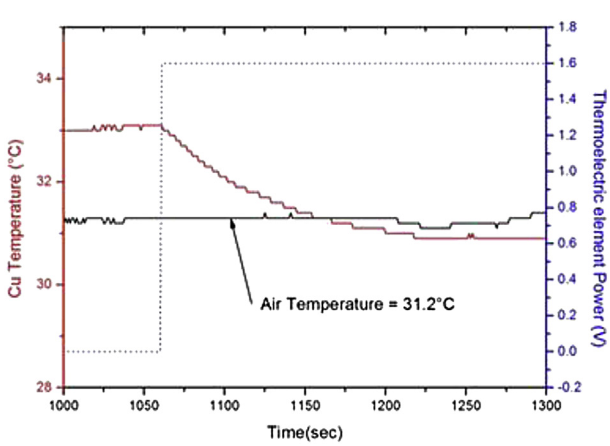

Fig. 19. Cooling performance with similar temperature of battery and flow field.

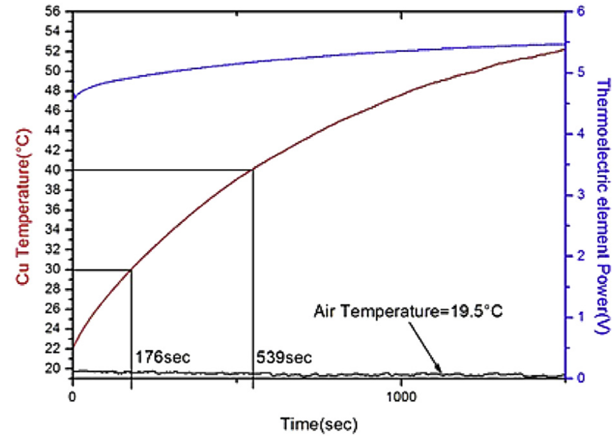

Fig. 20. Battery pre-heating performance with a TE device only.

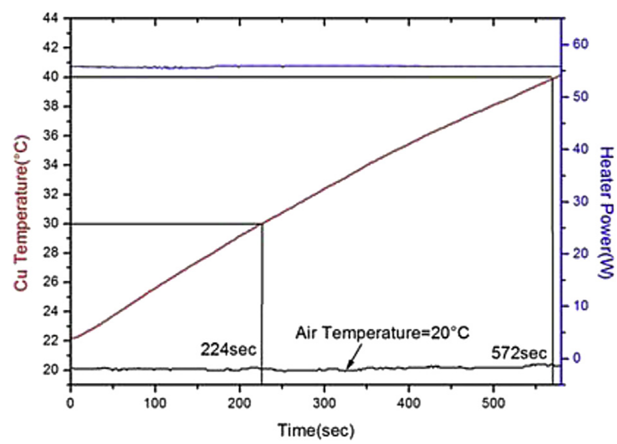

Fig. 21. Battery pre-heating with battery heater only.

Fig. 20 shows the test results when only the battery is heated (simulated condition due to actual operation) with 56 W without electrical supply to the TE device. When the flow field temperature is at 20 °C, the battery is heated to 30 °C in 224 s, and to 40 °C in 572 s.

In view of pre-heating during cold temperature start-up in typical winter operation, the TE device will speed up the start-up time by providing pre-heating for a cold battery, which will help the battery operation efficiency and reliability in practical

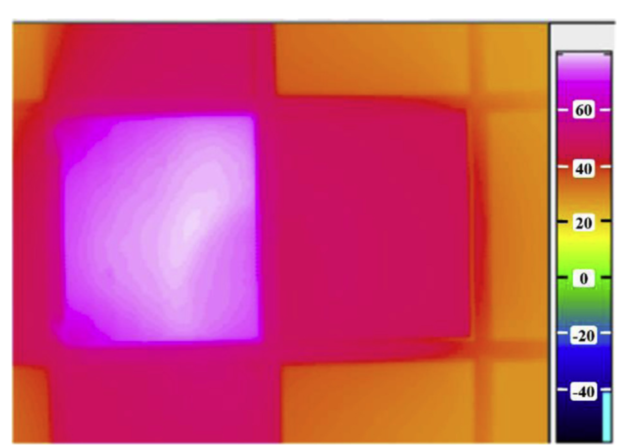

Fig. 22. Temperature distribution from an infrared camera during cooling by TE device.

application with a small amount of electrical energy to the TE device, as shown Fig. 21.

3.4. Test results with an infrared camera

The temperature distribution of the test setup was measured with an infrared camera when the battery is heated without the TE device being active, where the results are shown in Fig. 22.

The TE device temperature over the top side of the copper block of the center position shows higher temperature than the neighboring copper blocks because of the passive cooling effect of the TE device. These results verify the test set up modeling the battery heating behavior when heated to 60 °C.

Fig. 22 shows the temperature distribution when the TE device provides cooling. The TE temperature is higher than before, which means that the cooling heat from the battery actually heated up the TE device, as expected.

4. Conclusion

In this paper, a feasibility study was conducted to apply a thermoelectric device on a battery pack surface for cooling during summer and for pre-heating and waste heat recovery performance evaluation during winter. Based on the flow field and thermal field distribution from the simulation, it has been identified that the optimal flow and thermal field design are important in the battery operational efficiency, the charging and discharging performance, and eventually, the durability and reliability of the battery system, which are crucially important in the overall performance and reliability of electric vehicles.

By applying a thermoelectric device over the battery pack surface, the cooling effectiveness during summer, and the pre-heating and waste heat recovery performance during winter have been quantified through simulation and lab-environment experiment. It has been proved that the TE device over the battery pack in an electric vehicle provides a measurable amount of energy efficiency contribution with small input electrical energy, and more importantly, contributes to the battery operational efficiency and reliability. While intensive studies are performed to improve TE material properties, such as the Seebeck coefficient, the expected effectiveness with TE device will be higher than the results presented in this paper.

Acknowledgments

This research was supported by the Korean Ministry of Trade, Industry and Energy, through the Korea Evaluation Institute of Industrial Technology (Grant number: 10040133); by the Korean Ministry of Science, ICT and Future Planning through the National Research Foundation (Grant number: 2013R1A1A2009547).

References

[1] Tie SF, Tan CW. A review of energy sources and energy management system in electric vehicles. Renew Sustain Energy Rev 2013;20:82–102.
[2] Kumar S, Heister SD, Xu X, Salvador JR, Meisner GP. Thermoelectric generators for automotive waste heat recovery systems part 1 : numerical modeling and baseline model analysis. J Electron Mater 2013;42:4.
[3] Kumar S, Heister SD, Xu X, Salvador JR, Meisner GP. Thermoelectric generators for automotive waste heat recovery systems part 2: parametric evaluation and topological. J Electron Mater 2013;42:6.
[4] LeBlanc S, Yee SK, Scullin ML, Dame C, Goodson KE. Material and manufacturing cost considerations for thermoelectrics. Renew Sustain Energy Rev 2014;32:313–27.
[5] Boglietti A, Cavagnino A, Staton D, Shanel M, Mueller M, Mejuto C. Evolution and modern approaches for thermal analysis of electrical machines. IEEE Trans Ind Electron 2009;56:3.
[6] Pesaran AA. Battery thermal management in EVs and HEVs : issues and solutions. In: Advanced Automotive Battery Conference, Las Vegas, NV; 2001.
[7] Pesaran AA. Battery thermal models for hybrid vehicle simulations. J Power Sour 2002;110:377–82.
[8] Kim H, Park S-G, Jung B, Hwang J, Kim W. New device architecture of a thermoelectric energy conversion for recovering low-quality heat. Appl Phys A Mat Sci Process March 2014;114(4):1201–8.
[9] Mahamud R, Park C. Reciprocating air flow Li-ion battery thermal management to improve temperature uniformity. J Power Sour 2011;196: 5685–96.
[10] Tremblay O, Dessaint L-A, Dekkiche A-I. A generic battery model for the dynamic simulation of hybrid electric vehicles. In: IEEE Vehicle Power and Propulsion Conference; 2007. p. 284–9.
[11] Hsu C-T, Huang G-Y, Chu H-S, Yu B, Yao D-J. Experiments and simulations on low-temperature waste heat harvesting system by thermoelectric power generators. Appl Energy 2011;88:1291–7.
[12] Javani N, Dincer I, Naterer GF. Thermodynamic analysis of waste heat recovery for cooling systems in hybrid and electric vehicle. Energy 2012;46: 109–16.
[13] Gao X, Andreasen SJ, Chen M, Koer SK. Numerical model of a thermoelectric generator with compact plate-fin heat exchange for high temperature PEM fuel cell exhaust heat recovery. Int J Hydrogen Energy 2012;37:8490–8.
[14] Anderson JD. Computational fluid dynamics. 1st ed. McGraw-Hill; 1995.
[15] Versteeg HK, Malalasekera M. An introduction to computational fluid dynamics, the finite volume method. Prentice-Hall; 1996.
[16] CFD-ACE+ (ESI Group); 2004.
[17] CFX; 2004.
[18] Flow-3D (Flow Science, Inc.); 2004.
[19] Fluent Inc.. FLUENT; 2005.
[20] Glatzel T, Litterst C, Cupelli C, Lindermann T, Moosmann C, Niekrawietz R, et al. Computational fluid dynamics (CFD) software tools for microfluidic applications – a case study. Comput Fluid 2008;37:218–35.
[21] Lee T, Chambers B, Mahalingam Mali. Application of CFD technology to electronic thermal management. Components Packag Manuf Technol Part B Adv Packag IEEE Trans 1995;18(3):511–20.
[22] Negrao COR. Integration of computational fluid dynamics with building thermal and mass flow simulation. Energy Build 1998;27(4):155–65.
[23] Nelson P, Dees D, Amine K, Henriken G. Modeling thermal management of lithium-ion PNGV batteries. J Power Sour 2002;110:349–56.